

FIG. 2. Temperature distribution in chamber. Asterisks and triangles denote the temperatures of the upper boundary of the sensitive layer produced by a small and large number of condensation centers, respectively.

neutral, centers. Measurements have shown that the condensation on charged centers does not significantly affect the partial pressure distribution above the sensitive layer.

It was shown earlier² that the height of the sensitive layer changes with the temperature distribution inside the chamber. For any temperature distribution, the upper boundary of the sensitive layer can be established as being the section at which the temperature $T(x_0)$ has a value corresponding to the saturated vapor pressure $p_s(x_0) = p(x_0)/S_1$ where $p_s(x_0)$ is the pressure of the saturated vapor at a temperature $T(x_0)$, $p(x_0)$ is the partial pressure of the vapor at the upper boundary of the sensitive layer, and S_1 is the supersaturation at which condensation on the ions begins. As was mentioned earlier, measurements performed by the expansion method show that the pressure $p(x_0)$ is constant over a considerable volume of the chamber. Therefore, if we assume that a change in the temperature distribution does not affect substantially the partial pressure of the vapor above the sensitive layer, the upper boundary of the sensitive layer (where the supersaturation equals S_1) should have the same temperature regardless of the temperature distributions. This deduction is easily verified experimentally. Figure 2 shows five different temperature distributions. The temperature at which condensation on the ions begins is marked with an asterisk on each curve. It is apparent that the upper boundary of the sensitive layer actually has an approximately

constant temperature. Consequently, the assumption that in the region above the sensitive layer the partial pressure of the vapor does not change significantly with the temperature distribution is in agreement with the experimental data.

If the number of condensation centers inside the chamber increases (for example, when the chamber is irradiated by the gamma-ray source), the height of the sensitive layer decreases. The triangle on each temperature-distribution curve of Figure 2 designates the temperature of the upper boundary of the sensitive layer at which the ion concentration is thirteen times the initial concentration. It can be seen that the upper boundary of the sensitive layer remains at the same temperature as before for various temperature distributions. Decreasing the surface area of the evaporating liquid affects the variation in height of the sensitive layer in the same manner as increasing the ion concentration. The data given here shows that changing the condensation conditions over a wide range hardly affects the character of the partial pressure distribution above the sensitive layer.

In conclusion, I express my gratitude to M. S. Kozodaev and Professor M. F. Shirokov for interest in the work and for valuable comments.

¹ H. L. Morrison and G. I. Plain, *Rev. Sci. Instr.* **23**, 607 (1952)

² V. K. Lapidevskii and Iu. A. Shcherbakov, *J. Exper. Theoret. Phys. USSR* **27**, 103 (1954)

Translated by J. G. Adashko
190

The Problem of the Generalization of the Statistical Theory of the Atom

L. P. RAPOPORT

Voronezh State University

(Submitted to JETP editor March 1, 1955)

J. Exper. Theoret. Phys. USSR **29**, 376-377

(September, 1955)

THE known non-relativistic Hellman equations, generalizing the statistical theory of the atom for the case of electron groupings by the orbital numbers¹, can be generalized by incorporating relativistic and spin-orbital corrections for energy. In connection with the attempts made to use statistical methods for the calculation of the density of distribution of nucleons in nuclei²⁻⁴, the inclusion into these calculations of a term

which takes into account the spin-orbital interaction, and also the possibility of calculating the density of particles with a given orbital momentum represents particular interest.

We will consider the Dirac equation for the radial G and F functions in a centrally-symmetrical field with the potential V

$$\left(\frac{d}{dr} - \frac{1-k}{r}\right)G = \frac{1}{\hbar c}(E + eV + E_0)F, \quad (1)$$

$$\left(\frac{d}{dr} + \frac{1+k}{r}\right)F = \frac{1}{\hbar c}(E_0 - E - eV)G,$$

where $k = l + 1$ for $j = l + 1/2$; $k = -l$ for $j = l - 1/2$; $E_0 = mc^2$. Introducing new functions $g = rG$ and $f = rF$ and eliminating the function f from equations (1), for the function g we obtain

$$\frac{d^2 g}{dr^2} - \frac{k(k-1)}{r^2}g = \frac{E_0^2 - (E + eV)^2}{\hbar^2 c^2}g \quad (2)$$

$$+ \frac{e}{E_0 + E + eV} \frac{dV}{dr} \frac{dg}{dr}$$

$$- \frac{e}{E_0 + E + eV} \frac{k}{r} \frac{dV}{dr} g.$$

A comparison with the non-relativistic Schrödinger equation and an evaluation of the terms located on the right-hand side of Eq. (2), shows that the second term is much smaller than the remaining terms, and henceforward we will omit it.

We will now divide the atom into spherical layers of thickness s and we will consider s so small that in the layer under consideration V , $1/r^2$, $1/r$ remain constant. Then for the electron in this spherical layer we have

$$g_n = A \sin\left(n \frac{\pi r}{s} - n \frac{\pi r_k}{s}\right), \quad (3)$$

where r_k is the radius of the layer being considered, and $n = 1, 2, 3, \dots$

Substituting Eq. (3) in Eq. (2) and solving with respect to E , we obtain for the energy of the electron in the spherical layer in the state n :

$$E_n = E_0 \left\{ 1 + \left(\frac{\hbar}{mc}\right)^2 \right. \quad (4)$$

$$\left. \times \left(\pi^2 \frac{n^2}{s^2} + \frac{l(l+1)}{r^2} - \frac{e}{2E_0} \frac{k}{r} \frac{dV}{dr} \right) \right\}^{1/2} - eV,$$

where the substitution $k(k-1) = l(l+1)$ is made and it is assumed that $E_0 + E + eV \approx 2E_0$.

The first two terms in the round brackets of Eq. (4) represent the kinetic energy, and the third term the spin-orbital energy. The sum of these terms is considerably smaller than the rest energy of the electron E_0 . We will now consider that at any

definite l each of the states with $n = 1, 2, 3, \dots$ when the spin is taken into account has $2(2l+1)$ - multiple degeneration and that all the possible states are occupied. Then for the total (kinetic plus spin-orbital) energy W_k we obtain:

$$4\pi r^2 s W_k \approx \frac{\hbar^2}{2m} \sum_l \left\{ 2(2l+1) \frac{\pi^2}{s^2} \sum_1^n n^2 \right. \quad (5)$$

$$\left. + \frac{n^2(2l+1)l(l+1)}{r^2} \right\}$$

$$- \sum_l \frac{en(2l+1)}{4} \lambda_k^2 \frac{1}{r} \frac{dV}{dr}$$

$$+ (\text{relativistic corrections for the kinetic energy})$$

where $\lambda_k = \hbar/mc$.

In the statistical case, for large n , we have $\sum_1^n n^2 \approx \frac{n^3}{3}$; therefore, dividing Eq. (5) by $4\pi r^2 s$ and introducing the density of the electrons with a given l , $\rho_l = [2(2l+1)/4\pi r^2] (n/s)$, we obtain for the total energy E :

$$E = \sum_l \left\{ \frac{2\pi^2 \hbar^2 r^4}{3m(2l+1)^2} \rho_l^3 + \frac{\hbar^2 \cdot l(l+1)}{2m r^2} \rho_l \right. \quad (6)$$

$$\left. - \frac{1}{8} \lambda_k^2 \frac{e}{r} \frac{dV}{dr} \rho_l \right.$$

$$\left. + (\text{relativistic corrections}) - eV \rho_l \right\} \text{div.}$$

Varying Eq. (6) with respect to ρ_l with the additional condition $\int \rho_l dv = N_l$, where N_l is the total number of electrons in the atom with a given l , and neglecting the relativistic corrections for the kinetic energy, we obtain the expression for ρ_l , which, when substituted into the Poisson equation $\nabla^2 V = 4\pi e \sum \rho_l$, yields the Thomas-Fermi equation for the potential V :

$$\frac{d^2(rV)}{dr^2} = \frac{\sigma}{r} \sum_l (2l+1) \left\{ e(V - V_l) \right. \quad (7)$$

$$\left. + \frac{1}{8} \lambda_k^2 \frac{e}{r} \frac{dV}{dr} - \frac{\hbar^2}{2m} \frac{l(l+1)}{r^2} \right\}^{1/2},$$

where $\sigma = 2e\sqrt{2}/\pi\hbar$, V_l is the Lagrange multiplier. Equation (7) differs from the Hellman equation by an additional term which takes into account the spin-orbital interaction. The relativistic corrections for the kinetic energy were disregarded for simplicity.

It becomes possible to use the equation obtained for the calculation of the density of

nucleons in the nucleus, where the spin-orbital term is particularly significant.

¹ H. Hellman, *Acta Phys.-Chim. URSS* **4**, 225 (1936)

² D. Ivanenko and V. Rodichev, *Dokl. Akad. Nauk SSSR* **70**, 605 (1950)

³ P. Gombash, *Uspekhi Fiz. Nauk* **49**, 385 (1953)

⁴ L. Rapoport and V. Filimonov, *J. Exper. Theoret. Phys. USSR* **27**, 243 (1954)

Translated by E. Rabkin
209

Total Cross Sections of Nuclei of Certain Elements for Neutrons with Energies of 590 mev

V. P. DZHELEPOV, V. I. SATAROV AND
B. M. GOLOVIN

*Institute for Nuclear Problems,
Academy of Sciences, USSR*

(Submitted to JETP editor May 30, 1955)

J. Exper. Theoret. Phys. USSR **29**, 369-371
(September, 1955)

USING the synchrocyclotron of the Institute of Nuclear Problems we performed experiments for the purpose of determining the total cross section of protons, deuterons and more complex nuclei for neutrons with average effective energies of 590 mev. The neutrons were obtained as a result of "charge exchange" in beryllium of protons accelerated to energies of 680 mev. The above

cross sections were measured on the basis of the loss of neutrons from the beam.

The general experimental scheme is shown in Fig. 1. The absorbers of materials under investigation were placed immediately in front of the steel collimator (diameter of the aperture: 3cm) which was placed within the protective wall. The neutrons, having traversed the absorber and the collimator were detected by the telescope T_1 , composed of three scintillation counters (with tolane crystals) which registered the recoil protons emitted at an angle of 20 degrees from a polyethylene scatterer placed in the beam. The experiments were performed under conditions of good geometry. The neutrons scattered in the sample at an angle greater than 15 minutes could not strike the scatterer and consequently were not detected by the telescope. The intensity of the neutron beam was continuously controlled by means of a similar telescope T_2 . The resolving time of coincident events of the telescopes was 6×10^{-8} sec.

The energy threshold of the detector for neutrons was 470 mev, determined by the thickness of tungsten filters placed between the second and third counters. The neutron energy distribution in the beam was determined in our laboratory by Fliagin¹. The results of these measurements are shown in Fig. 2. With the energy threshold of the detector set to the above indicated value, the average effective energy of the neutrons for which we determined the cross sections, $E_{n, \text{average}}^{\text{eff}} = 590$ mev. The cross sections were determined on the basis of the formula:

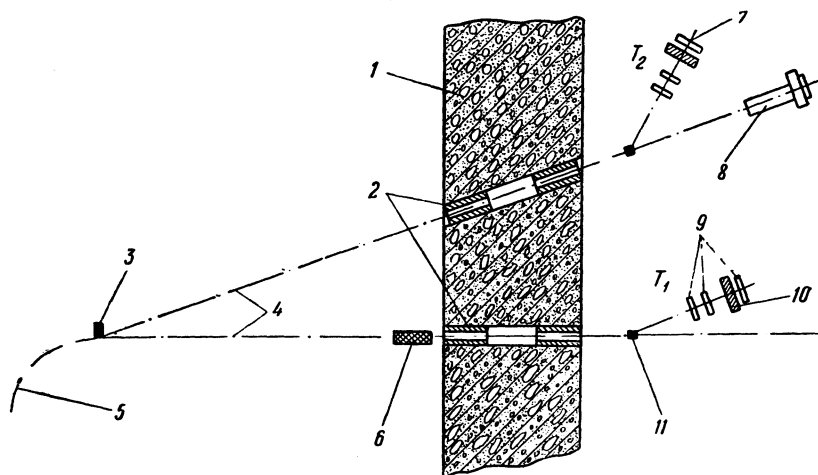


FIG. 1. Experimental Arrangement. 1 - Concrete shield; 2 - Collimators; 3 - Target (Be); 4 - Neutrons; 5 - Protons ($E_p = 580$ mev); 6 - Sample; 7 - Telescope; 8 - Bi-Chamber; 9 - Detecting telescope; 10 - Filter; 11 - Scatterer